NASA TECHNICAL NOTE

NASA TN D-3712

NASA TN D-3712

c. 1

USE OF ANALOG COMPUTATION IN PREDICTING DYNAMIC TEMPERATURE EXCURSIONS OF ORBITING SPACECRAFT

by Frank J. Cepollina

Goddard Space Flight Center
Greenbelt, Md.

NATIONAL AERONAUTICS AND SPACE ADMINISTRATION • WASHINGTON, D. C. • FEBRUARY 1967

USE OF ANALOG COMPUTATION IN PREDICTING DYNAMIC TEMPERATURE EXCURSIONS OF ORBITING SPACECRAFT

By Frank J. Cepollina

Goddard Space Flight Center
Greenbelt, Md.

NATIONAL AERONAUTICS AND SPACE ADMINISTRATION

For sale by the Clearinghouse for Federal Scientific and Technical Information
Springfield, Virginia 22151 – Price $1.00

ABSTRACT

Presented herein is an analog computer program capable of predicting an orbiting spacecraft's external surface temperatures. By dividing a spacecraft's external surface into sections and applying transient heat transfer and thermodynamic equations to the boundaries of each section, an analog circuit describing the total incident energy as a function of spacecraft orbital position is written. The source of the external incident energy simulated can be from any combination of solar radiation, earth albedo, earth thermal emission, solar paddle emission and reflection. The sources of internal energy incident to the inner surfaces can be from instrument power dissipation, and from radiation interchange between adjacent and opposite surfaces. Using the AOSO proposed spacecraft as the thermal model, the analog computer solution is shown for the parameters involved.

CONTENTS

USE OF ANALOG COMPUTATION IN PREDICTING DYNAMIC TEMPERATURE EXCURSIONS OF ORBITING SPACECRAFT

by
Frank J. Cepollina
Goddard Space Flight Center

INTRODUCTION

An analog computer program suitable for the analysis and design of spacecraft thermal control systems is described. The program was written essentially for the Advanced Orbiting Solar Observatory (AOSO) configuration; however, it can easily be adjusted to handle a multitude of configurations and orbital conditions. Given a set of thermal properties and orbital thermal flux, the program will yield skin temperatures as a function of the spacecraft orbital position. If optimum spacecraft surface thermal properties are desired so as to minimize temperature excursions, the program will yield the optimum thermal properties to achieve minimum temperature excursions. In addition, the program is capable of solving internal temperature gradients across instrument packages, structural members, and thermal insulation materials as a function of spacecraft orbital position. Thus, detrimental temperature gradients resulting from various modes of operation (occulted, standby, failure) and various patterns of energy dissipation (on-off operation of instruments, batteries, and controls) can be predicted, and optimization of the thermal design achieved through the use of this program.

THE PROGRAM MODEL

The basic capabilities of the differential analog computer are the solution of ordinary differential equations. A typical spacecraft thermal analysis problem falls within the scope of these capabilities. Taking the AOSO spacecraft (4-solar paddle configuration) as an example (Figure 1), the cylindrical outer surface is sectioned by system boundaries, as shown in Figure 2. Each section of surface receives external environment thermal flux and internal dissipated energy, while simultaneously exchanging energy through reflection, emission, and conduction with space, spacecraft appendages, and the remaining sections of surface. The general differential energy balance equation, which can be written for each section, follows.

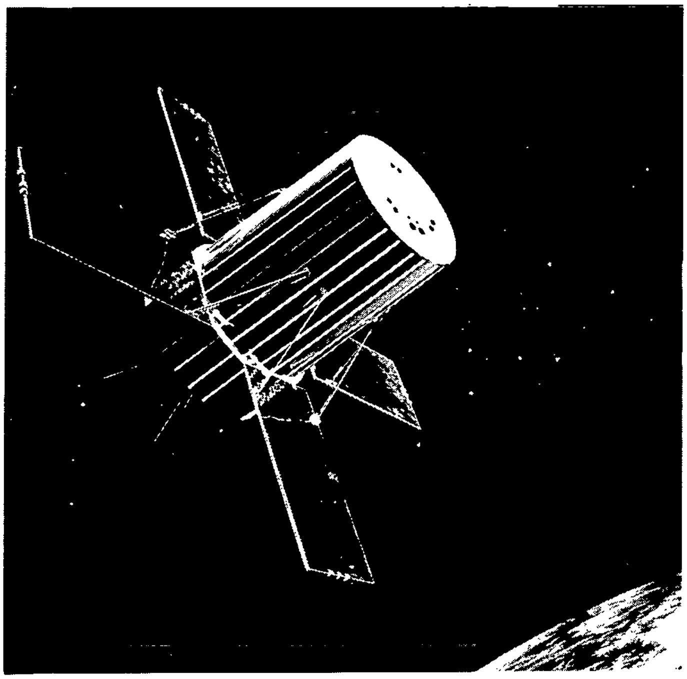

Figure 1— Three-axis stabilized cylindrical spacecraft (AOSO).

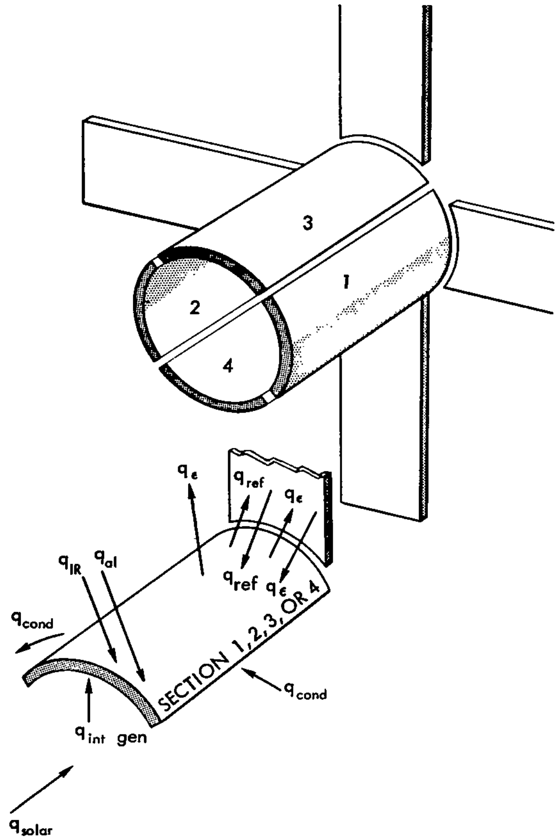

Figure 2—Thermal model of a cylindrical spacecraft.

$$WC_P \frac{dT}{d\tau} = Q_{ap} \quad + \quad q_{int} \quad + \quad \epsilon_s F_\epsilon (f_p) A_s E_t \quad + \quad \alpha_s F_p (f_p) A_p S$$

Solar energy entering through apertures

Internal energy generated by electrical dissipation

Earth emission flux absorbed by each section as a function of orbit position and time

Earth albedo flux absorbed by each section as a function of orbit position and time

$$+ \quad [\rho_{sp} \alpha_s F_v A_p S \quad + \quad (F_{ps})_{gr} A_s \sigma (T_{ps}^4 - T_s^4)]$$

Solar normal energy reflected from solar paddles and absorbed by section

Net thermal radiation exchange from paddles to section

$$-\epsilon_s A_s \sigma (T_s^4 - T_{space}^4) \quad \pm \quad \Sigma q_{cond} \quad \pm \quad \Sigma q_{rad\ int},$$

Total thermal emission to space from each section

Net sum of all energy conducted to or from each section

Net sum of all energy radiated to or from each sections internal surface where

$W \equiv$ Mass of the cylindrical section (thermal shield section),

$C_p \equiv$ Specific heat of section material,

$Q_{ap} \equiv$ Solar energy entering through lens apertures on solar normal face,

$\epsilon_s \equiv$ External surface emissivity of thermal shield,

$F_\epsilon \equiv$ Earth to spacecraft thermal emission form factor—a function of spacecraft orbit and location in orbit (f_p),

$A_s \equiv$ Surface area of each section of the thermal shield,

$E_T \equiv$ Earth thermal emission (average) = 66.38 BTU/hr-ft^2,

$\alpha_s \equiv$ External surface solar absorptivity of thermal shield,

$F_p \equiv$ Earth to spacecraft form factor for earth albedo—a function of spacecraft orbit and position in orbit with respect to the earth (f_p),

$A_p \equiv$ Projected area of each section of thermal shield,

$S \equiv$ Solar constant = 443 BTU/hr-ft^2,

$\sigma \equiv$ Stefan Boltzmann's natural constant = 0.178×10^{-8} BTU/hr-ft^2 (°R)^4,

$\rho_{sp} \equiv$ Solar reflectivity of solar paddles,

$F_v \equiv$ Geometric form factor between solar paddles and each thermal shield section,

$(F_{pRs})_{gr} \equiv$ Gray body configuration factor for thermal emission between paddle and thermal shield section,

$T_{ps} \equiv$ Temperature of paddle surface,

$T_s \equiv$ Temperature of thermal shield section; for each section T_{s1}, T_{s2}, T_{s3}, $T_{s4} \equiv T_1$, T_2, T_3, T_4 respectively,

$T_{space} \equiv$ Temperature of space, assumed equal to zero °R,

$q_{cond} \equiv$ Thermal conduction to or from each thermal shield section,

$q_{rad\ int} \equiv$ Net emission exchange from the internal surface of each thermal shield section.

ASSUMPTIONS

The analysis presented in this report for purposes of illustration is based on the AOSO configuration and its parameters, including:

1. The AOSO cylindrical spacecraft, 4-paddle configuration.
2. The AOSO orbit (300 nm near-polar orbit):
   a. Continuous solar pointing spacecraft
   b. Space-oriented three-axis stabilized spacecraft.
3. Analog approximation of the earth albedo and IR flux curves as computed by the digital orbital mechanics program.
4. Other assumptions as noted throughout the report.

MECHANIZATION OF THERMAL MODEL

For each thermal system boundary section of Figure 2, the general differential equation is rewritten in terms of coefficients and variables (References 1 and 2) and with the sign convention that energy entering a system boundary is negative and that leaving is positive.*

For Section 1,

$$- W_1 C_p \frac{dT}{d\tau} = - A_1 - B_1 - C_1(f_p) - D_1(f_p) - E_1 - F_1(T^4_{ps1} - T^4_{s1}) + G_1(T^4_{s1}) + \Sigma q_{cond_{(1-3),(1-4)}} + \Sigma q_{rad_{(1,2,3,4)}} \cdot \quad (1)$$

For Sections 2, 3, and 4, the following equation applies,

$$-\left(W C_p \frac{dT}{d\tau}\right)_{2,3,4} = - A_{2,3,4} - B_{2,3,4} - C_{2,3,4}(f_p) - D_{2,3,4}(f_p) - E_{2,3,4}$$

$$- F_{2,3,4}(T^4_{ps\,2,3,4} - T^4_{s\,2,3,4}) + G_{2,3,4}(T^4_{s\,2,3,4}) + \Sigma q_{cond_{2,3,4}} + \Sigma q_{rad_{2,3,4}} \cdot \quad (2)$$

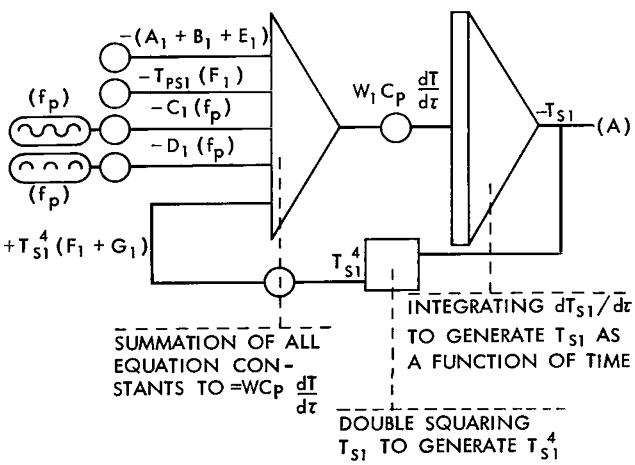

Figure 3—Basic circuit for each section.

The constant coefficients of these equations are $A_{1,2,3,4}$; $B_{1,2,3,4}$; $E_{1,2,3,4}$; $F_{1,2,3,4}$, and $G_{1,2,3,4}$. The variable coefficients are $C_{1,2,3,4}(f_p)$ and $D_{1,2,3,4}(f_p)$. Both of the variable coefficients are dependent on the specific spacecraft orbit and the position of the spacecraft in that orbit (relative to the earth) at any instant of time. Each of the above equations can therefore be mechanized by the following differential analog circuit (Figure 3).

By using four analog circuits identical to that in Figure 3, (one for each of the four system boundaries equations), it is possible to

*This sign inversion facilitates efficient analog mechanization of the general equations and insures solution stability as per Rouths criterion (Reference 3).

generate the temperatures of each of the four sections as a function of time. However, the resulting temperatures would be generated independently of any conduction or internal radiation exchange between sections and internal components of the spacecraft. In reality, spacecraft do interchange energy across these theoretical system boundaries via conduction and internal radiation. Therefore, it is essential that a means of conduction and radiation coupling between each of the four circuits be included in the program.

Conductive Coupling

The net thermal energy conducted to any section is a function of the temperature difference between any given section and its adjacent sections.

For example, for Section 1, if the thermal conduction resistance, R, is assumed equal for each of the four system boundaries, then

$$\Sigma q_{cond_1} = -\frac{1}{R}(T_4 - T_1) + \frac{1}{R}(T_1 - T_3)$$

$$= \frac{2}{R} T_1 - \frac{1}{R} T_4 - \frac{1}{R} T_3 \quad . \tag{3-1}$$

Similarly, for Sections 2, 3, and 4,

$$\Sigma q_{cond_2} = \frac{2}{R} T_2 - \frac{1}{R} T_3 - \frac{1}{R} T_4 \ , \tag{3-2}$$

$$\Sigma q_{cond_3} = \frac{2}{R} T_3 - \frac{1}{R} T_1 - \frac{1}{R} T_2 \ , \tag{3-3}$$

$$\Sigma q_{cond_4} = \frac{2}{R} T_4 - \frac{1}{R} T_1 - \frac{1}{R} T_2 \ . \tag{3-4}$$

By incorporating the above equations into four circuits (each identical to the circuit described in Figure 3), conductive coupling of each section is accomplished. The mechanization of the equation is achieved through the use of feedback loops (Reference 3), and the resulting interconnected circuits are described in Figure 4.

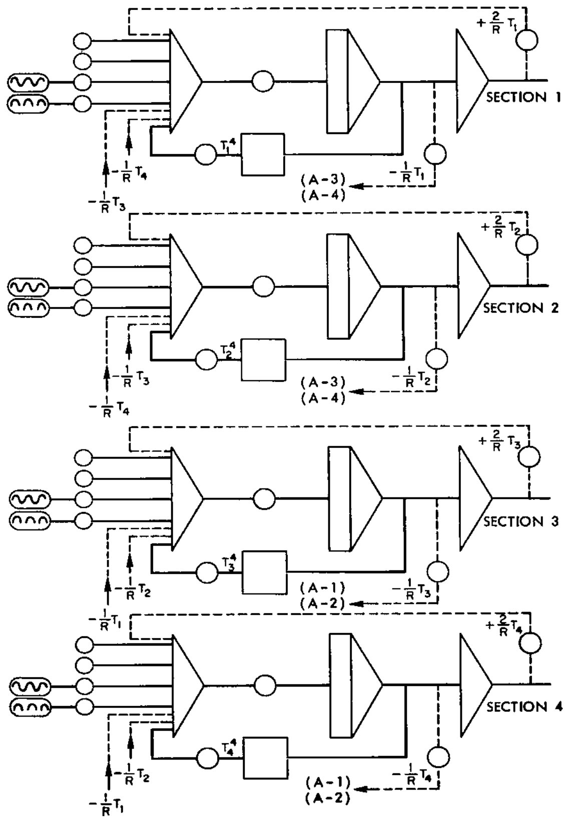

Figure 4—Basic circuit diagram with conduction coupling.

Internal Radiation Coupling

The technique used to incorporate internal radiation coupling into the program is very

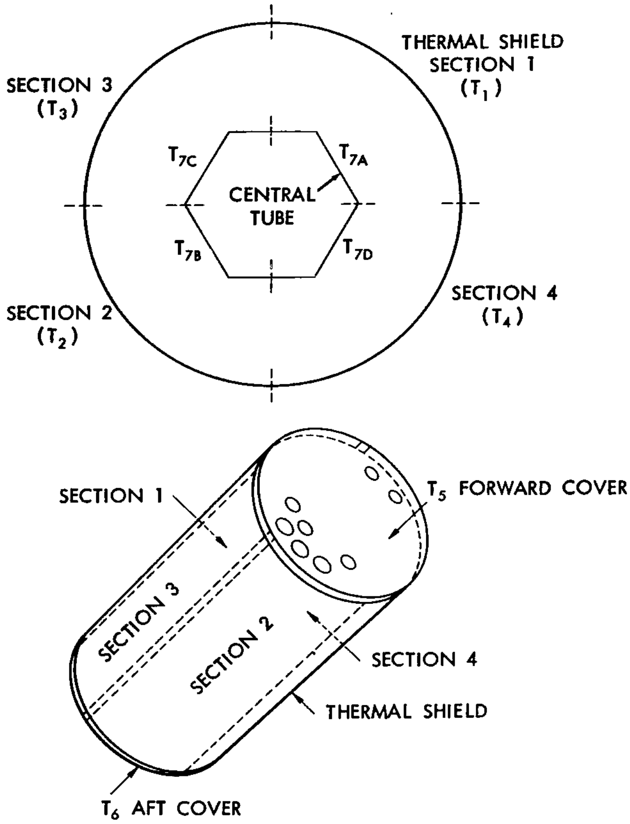

Figure 5—Internal thermal model.

much the same as that used to achieve conductive coupling. A simplified internal configuration of the spacecraft experiment compartment is used to demonstrate the technique. Figure 5 illustrates the thermal shield (with the four arbitrary system boundaries and a hexagonal central support column or tube). In addition, a solar normal cover and an aft cover are added to the thermal model. Both forward and aft covers are assumed to be at constant temperatures, and conductively insulated from the thermal shield. These assumptions reduce the complexity of the program, but are not requirements to the operation of the program.

The net radiation exchange to Section 1 from all other sections, central tube, and forward and aft covers, can be expressed by the equation

$$
\begin{aligned}
q_{rad_1} &= F_{14} A\sigma (T_1^4 - T_4^4) + F_{13} A\sigma (T_1^4 - T_3^4) \\
&+ F_{12} A\sigma (T_1^4 - T_2^4) + F_{15} A\sigma (T_1^4 - T_5^4) \\
&+ F_{17} A\sigma (T_1^4 - T_7^4) + F_{16} A\sigma (T_1^4 - T_6^4) \\
&+ F_{16} A\sigma (T_1^4 - T_{7A}^4) \, .
\end{aligned} \tag{4}
$$

For the particular configuration, F_{12} is approximately equal to zero and by symmetry, $F_{13} = F_{14}$ and $F_{15} = F_{16}$. Combining and expanding terms yields the following equation:

$$
\begin{aligned}
\Sigma\, q_{rad_1} &= F_{14} A_1 \sigma (2 T_1^4 - T_4^4 - T_3^3) \\
&+ F_{15} A_1 \sigma (2 T_1^4 - T_5^4 - T_6^4) \\
&+ F_{17} A_1 \sigma (T_1^4 - T_{7A}^4) \, .
\end{aligned} \tag{4-1}
$$

By analogy, each of the remaining section equations are written

$$
\begin{aligned}
\Sigma\, q_{rad_2} &= F_{24} A_2 \sigma (2 T_2^4 - T_4^4 - T_3^4) \\
&+ F_{25} A_2 \sigma (2 T_2^4 - T_5^4 - T_6^4) \\
&+ F_{27} A_2 \sigma (T_2^4 - T_{7B}^4) \, ,
\end{aligned} \tag{4-2}
$$

$$\Sigma q_{rad_3} = F_{31} A_3 \sigma (2 T_3^4 - T_2^4 - T_1^4)$$

$$+ F_{35} A_3 \sigma (2 T_3^4 - T_5^4 - T_6^4)$$

$$+ F_{37} A_3 \sigma (T_3^4 - T_{7C}) , \qquad (4\text{-}3)$$

and

$$\Sigma q_{rad_4} = F_{41} A_4 \sigma (2 T_4^4 - T_1^4 - T_2^4)$$

$$+ F_{45} A_4 \sigma (2 T_4^4 - T_5^4 - T_6^4)$$

$$+ F_{47} A_4 \sigma (T_4^4 - T_{7D}^4) . \qquad (4\text{-}4)$$

To implement placing these equations into the circuits of Figure 4, the technique of feedback loops is again used. However, at this point no circuit exists to generate T_{7A}, T_{7B}, T_{7C}, T_{7D}, T_5 and T_6. If it is assumed that these values are known constants, then mechanization can proceed. If they are known independent variables, then a function generation of the independent variables is required as inputs to the circuits of Figure 4. On the other hand, if they are unknown dependent variables (functions of the temperature and energy received from the surroundings), then it is necessary to write additional differential equations and mechanize circuits to generate these variables. The technique used to write and mechanize the additional equations is identical to that described in the preceding pages.

So as not to confuse the illustration of the analog computation technique, the terms $T_{7A,B,C,D}$, T_5 and T_6 shall be considered constant, even though it is not a requirement to the analog solution.

Figure 6 illustrates the mechanization of these radiation coupling equations, 4-1, 4-2,

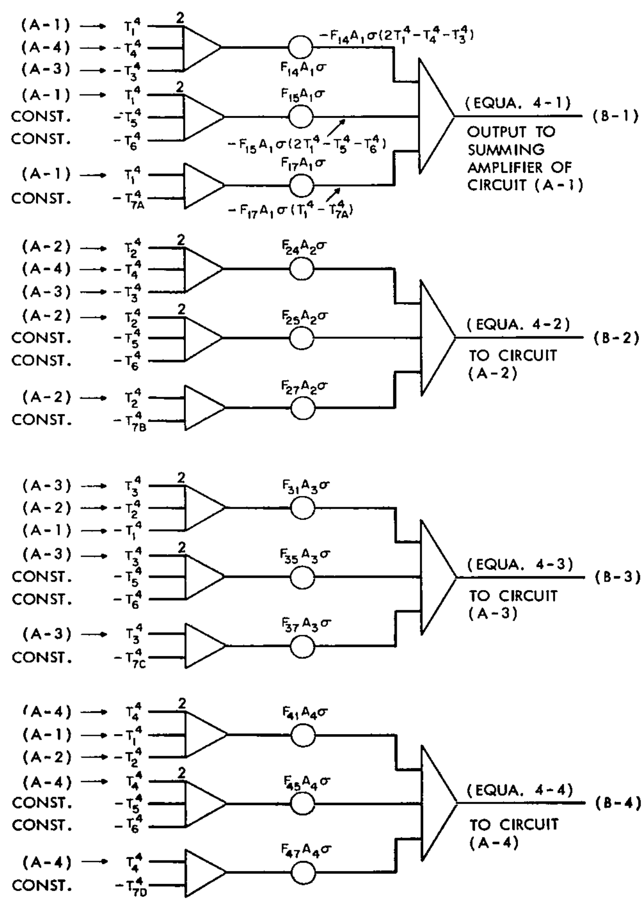

Figure 6—Mechanization of radiation coupling equations.

4-3, and 4-4. Note that for circuit B-1, T_1^4, T_4^4, and T_3^4, functions are generated by circuits A-1, A-4, and A-3, respectively. Multiplication by factors of two of the T_1^4 function is achieved by using gains of two at each respective summing amplifier input. By assumption, T_5^4, T_6^4, and T_{7A}^4 are constants. Now, by taking the output of the final summing amplifier and inputting this into the summing amplifier of circuit A-1, the radiation exchange (coupling) loop is completed for Section 1. By the identical procedure, radiation coupling is accomplished for Sections 2, 3, and 4. Figure 7 illustrates the augmentation of radiation coupling into the main circuits.

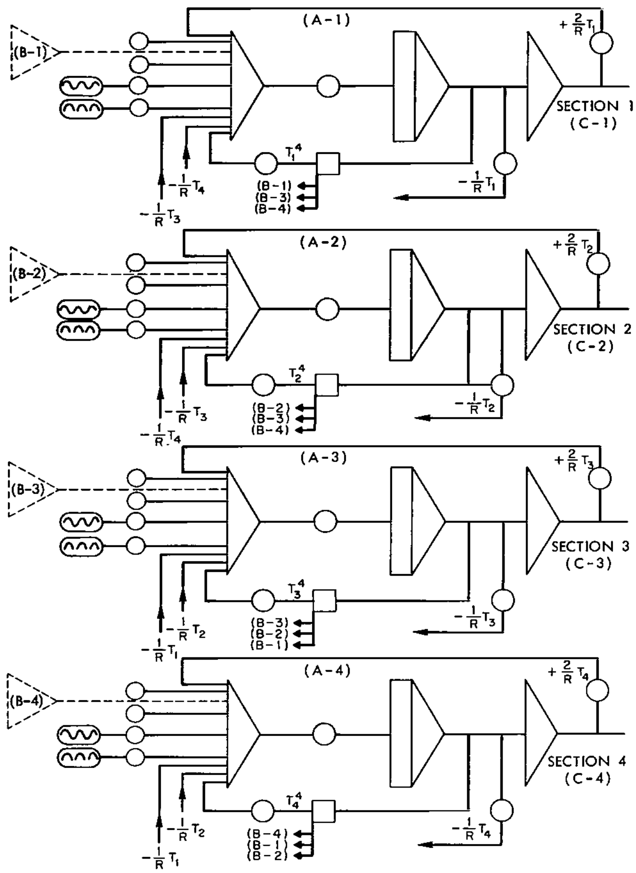

Figure 7—Circuit diagram incorporating both radiation and conduction coupling.

SIMULATION OF TIME VARYING HEAT FLUXES

The generation of earth thermal emission and earth albedo heat flux is accomplished by simulation rather than by solution of the orbital mechanics equations. Although it is possible to solve these equations by analog techniques, the higher degree of accuracy of digital computation techniques cannot be disputed. Therefore, this particular technique simulates the time varying heat flux as predicted from the digital orbital mechanics program.

The approach taken to develop the simulation is as follows (Reference 4):

1. Write the Fourier Series expression which approximates the shape of the albedo and IR flux curves for each of the four boundary sections.

2. Compute the amplitude and phase shift required for each flux curve for each of the four sections.

3. Mechanize a single cosine/sine generation circuit.

4. Mechanize each of the Fourier expressions through the use of diode chopped feedback amplifiers and the single sine/cosine circuit.

5. The potentiometer settings are then adjusted so that the output of each amplifier matches its respective digital flux curve. For the ease of making rapid changes in the external emissivity, ϵ, and solar absorbtivity, α, of each spacecraft section, a separate row of potentiometers is placed in the circuit.

Figure 8 illustrates two flux generation circuits coupled to a single sine/cosine generation circuit. Figures A1, A2, A3, and A4 of Appendix A present the simulated earth emission and albedo fluxes for each of the four sections of spacecraft surface. To demonstrate the accuracy of the simulation, a comparison is made between computed digital values of flux (Reference 5) and the values simulated by the flux generation circuits (for each of the four surface sections). As can be seen in the referenced figures, the simulation can be made to match the digital solution closely. The circuits which generate these time varying fluxes are shown in Figure A5 of Appendix A.

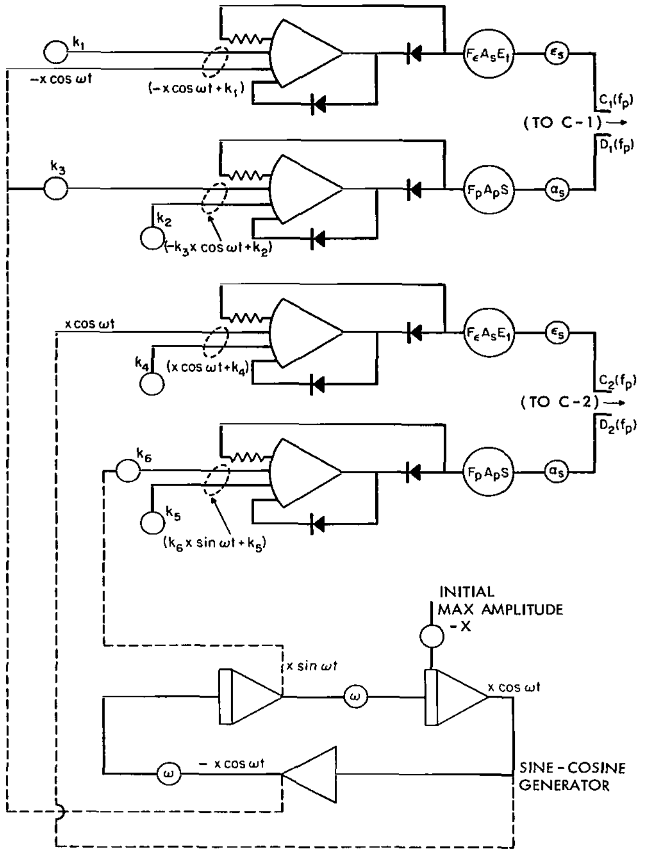

Figure 8—Sample earth thermal flux simulation circuits.

TEMPERATURE ANALYSIS (COMPUTER RUNS)

The circuit diagram of Figure A5, Appendix A, represents the complete mechanization of the preceding equations into a differential analog computer program. Through the use of this circuit, the program is demonstrated. The particular temperature analysis (computer runs) is made for a cylindrical, 48-inch diameter, solar pointing, three-axis stabilized spacecraft in a 300 nm near-polar orbit. The sample evaluation of equation constants, coefficients, and scaling is included in Appendix A. The earth flux condition is taken as the summer solstice (June 21) orbital period. The simulated flux for each node is described in Appendix A, Figures A1, A2, A3, and A4.

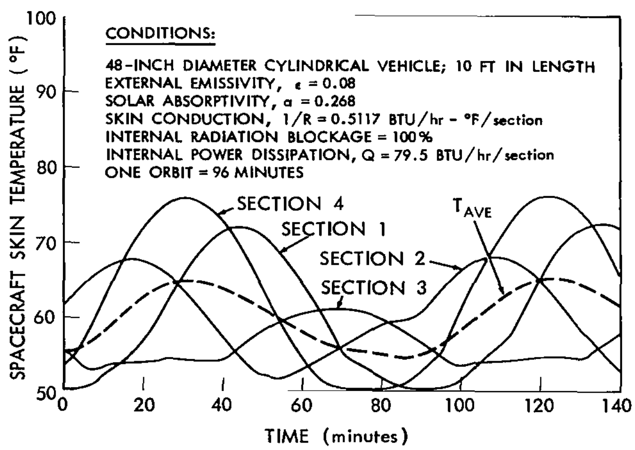

Figure 9—Analog computer run for thermal design optimization.

The following figures illustrate computer solutions for various enumerated thermal properties of the spacecraft's surface (Figures 9, 10, 11, and 12).

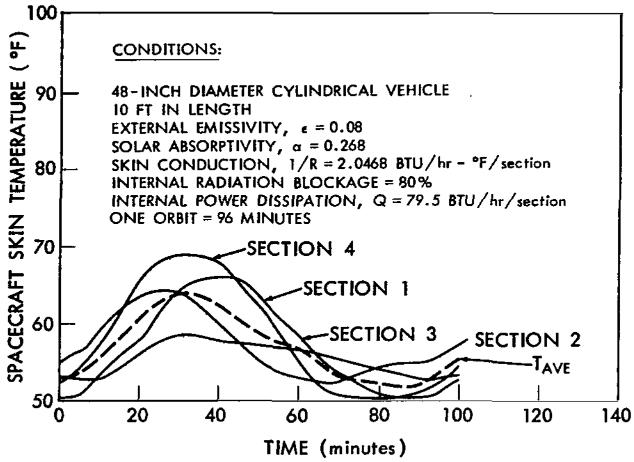

Figure 10—Analog computer run for thermal design optimization.

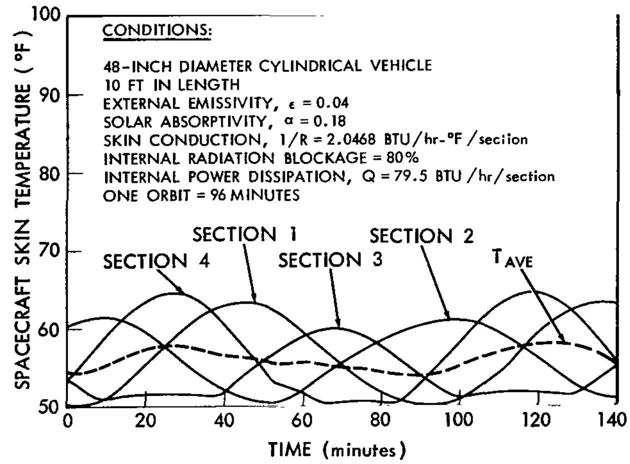

Figure 11—Analog computer run for thermal design optimization.

CONCLUSION

The basic capabilities of the analog computer comprise the solution of ordinary differential equations. A typical spacecraft thermal analysis problem falls within the scope of these capabilities. Using the proposed Advanced Solar Observatory as an example, thermal analysis solutions have been demonstrated. The thermal model consisted of the spacecraft's cylindrical surface sectioned by systems boundaries, and the general differential energy balance equations were written for each boundary section. It has been further demonstrated that a differential analog circuit can be designed to generate the solution of each differential energy balance equation. Time varying orbital flux can also be accurately simulated, and the flux simulating circuits were designed so that thermal properties (surface emissivity, absorptivity, form factors) can be readily varied to accommodate rapid optimization of thermal properties. Finally, several analog runs were made to demonstrate the capabilities of the program.

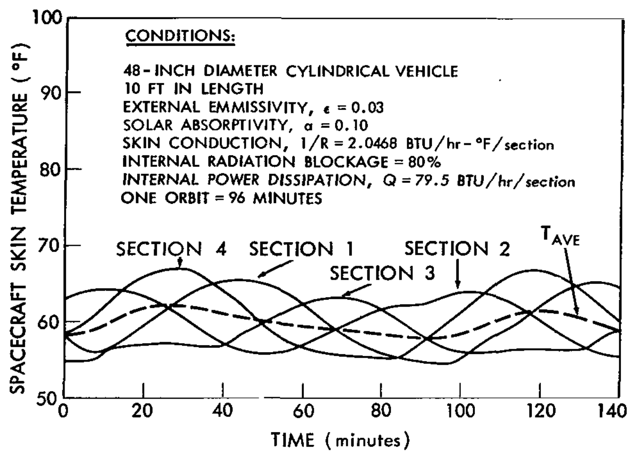

Figure 12—Analog computer run for thermal design optimization.

Goddard Space Flight Center
National Aeronautics and Space Administration
Greenbelt, Maryland, May 2, 1966
829-11-75-01-51

REFERENCES

1. Kreith, F., "Radiation Heat Transfer for Spacecraft and Solar Power Plant Design," New York: International Textbook Company, 1962.

2. Powers, E. I., "Thermal Radiation to a Flat Surface Rotating About an Arbitrary Axis in an Elliptical Earth Orbit: Application to Spin Stabilized Satellites," NASA Technical Note D-2147, April 1964.

3. Rodgers, A. E., and Connoly, T. W., "Analog Computation in Engineering Design," New York: McGraw Hill Book Company, 1960.

4. Jackson, A. S., "Analog Computation," New York: McGraw Hill Book Company, 1960.

5. Stevenson, J. A., and Grafton, J. C., "Radiation Heat Transfer Analysis for Space Vehicles," Aeronautical Systems Division Technical Report 61-119, U. S. Air Force, December 1961.

Appendix A

Sample Preparation of Input Data for Spacecraft Temperature Analysis by Differential Analog Computer

General Equation

For a three-axis stabilized spacecraft, cylindrical in configuration, solar pointing in orientation, and in a 300 nm near-polar orbit, the following general equation applies:

$$\left(WC_p \frac{dT}{d\tau}\right)_{1,2,3,N} = A_{1,2,3,N} + B_{1,2,3,N} + C_{1,2,3,N}(f_p) + D_{1,2,3,N}(f_p) + E_{1,2,3,N} + F_{1,2,3,N}(T^4_{ps\,1,2,3,N} - T^4_{s\,1,2,3,N})$$

$$- G_{1,2,3,N}\,(T^4_{s\,1,2,3,4}) \pm \Sigma\, q_{cond_{1,2,3,4}} \pm \Sigma\, q_{rad\ int_{1,2,3,N}}\,. \qquad \text{(A1)}$$

The subscripts 1, 2, 3, and N represent the number of respective equations for N thermal boundary sections (nodes) comprising a spacecraft thermal model. If the spacecraft's shell is cylindrical[1] and is divided into four thermal boundary sections, then four equations identical to Equation A1 will describe the temperature history of the spacecraft's shell. Since each equation is identical for the cylindrical thermal model being studied, only the evaluation of one equation describing one section (node) will be discussed herein (the technique being the same for each remaining equation).

Evaluation of Terms

For the aforementioned three-axis stabilized spacecraft, the constant terms of Equation A1 are

$A \equiv Q_{AP}$, solar energy absorbed through apertures,

$B \equiv q_{int}$, internal electrical power dissipation,

and

$E \equiv$ Solar paddle reflections absorbed by skin section.

The equation independent variable terms are

$C(f_p) \equiv$ Incident earth IR flux (simulated functions of sin and cos of θ),

and

$D(f_p) \equiv$ Incident earth albedo flux (simulated functions of sin and cos of θ).

The equation dependent variable terms are

$F(T_{ps}^4 - T_s^4) \equiv$ Paddle-to-skin IR exchange,

$G(T_s^4) \equiv$ Skin surface emission to space,

$\Sigma q_{cond} \equiv$ Skin section conduction,

$\Sigma q_{rad\ int} \equiv$ Skin section internal radiation exchange,

and

$dT/d\tau \equiv$ Transient change in temperature of a section with respect to time.

The computer variables of Equation A1, Section 1, are

Equation Variables	Computer Variables
$\frac{dT_{s1}}{d\tau}$	$\dot{T}_{s1}$
T_{s1}, T_{s3}, T_{s4}	T_{s1}, T_{s3}, T_{s4}
$T_{s1}^4, T_{s3}^4, T_{s4}^4$	$T_{s1}^4, T_{s3}^4, T_{s4}^4$
θ	ωt

Computer Equation

Rewriting Equation A1 in terms of the computer variables and using the sign convention that energy entering a system boundary is negative and that leaving is positive, yields

$$
\begin{aligned}
-WC_p[\dot{T}_{s1}] = {} & -A_1 - B_1 - E_1 - C_1(f_p[\cos\omega t]) - D_1(f_p[\cos\omega t]) + (F+G)[T_{s1}^4] \\
& - F(T_{ps1}^4) + \frac{1}{R_{cond}}(2[T_{s1}] - [T_{s4}] - [T_{s3}]) \\
& + \frac{1}{R_{rad_1}}(2[T_{s1}^4] - [T_{s4}^4] - [T_{s3}^4]) \\
& + \frac{1}{R_{rad_2}}(2[T_{s1}^4]) - \frac{1}{R_{rad_2}}(T_5^4 - T_6^4) \\
& + \frac{1}{R_{rad_3}}[T_{s_1}^4] - \frac{1}{R_{rad_3}}(T_{7_A}^4) \, . \qquad \text{(A2)}
\end{aligned}
$$

Inputting values from Table 1 into Equation A2 yields the following unscaled computer equation:

$$
\begin{aligned}
-4.8\,[\dot{T}_s] = & -267.33 - 63.44\,\{f_p\,[\cos \omega t]\} - 48.33\,\{f_p\,[\cos \omega t]\} \\
& + 0.3741 \times 10^{-8}\,\{[T_{s_1}^4]\} + 0.5117\,\{2\,[T_{s_1}] - [T_{s_4}] - [T_{s_3}]\} \\
& + 0.3988 \times 10^{-8}\,\{2\,[T_{s_1}^4] - [T_{s_4}^4] - [T_{s_3}^4]\} \\
& + 0.3551 \times 10^{-8}\,\{2\,[T_{s_1}^4] - 2(520)^4\} + 0.8915 \times 10^{-8}\,\{[T_{s_1}^4] - (520)^4\} \,. \qquad \text{(A3)}
\end{aligned}
$$

The amplitude scaled equation is

$$
\begin{aligned}
-0.48[\dot{T}_{s1}] = & -26.73 - 6.344\,\{f_p\,[\cos \omega t]\} - 4.833\,\{f_p\,[\cos \omega t]\} + 0.03741\left\{(10^{-4})\left[\left(\frac{T_{s1}}{10}\right)^4\right]\right\} \\
& + 0.05117\left\{\left[\frac{T_{s1}}{10}\right] - \left[\frac{T_{s4}}{10}\right] - \left[\frac{T_{s3}}{10}\right]\right\} \\
& + 0.03998\left\{(2 \times 10^{-4})\left[\left(\frac{T_{s1}}{10}\right)^4\right] - (10^{-4})\left[\left(\frac{T_{s4}}{10}\right)^4\right] - (10^{-4})\left[\left(\frac{T_{s3}}{10}\right)^4\right]\right\} \\
& + 0.03551\left\{(2 \times 10^{-4})\left[\left(\frac{T_{s1}}{10}\right)^4\right]\right\} - 51.8 \\
& + 0.08915\left\{(10^{-4})\left[\left(\frac{T_{s1}}{10}\right)^4\right]\right\} - 65.0 \,. \qquad \text{(A4)}
\end{aligned}
$$

Time scaling the computer integration and earth flux generation rates,

$$\frac{T}{10} = 0.48\,\frac{dT}{d\tau} \,,$$

$$\frac{T}{10} = \frac{0.1}{0.48}\,[0.48\dot{T}] \,,$$

$$\frac{T}{10} = 0.20833\,[0.48\dot{T}]\ {}^{\circ}\mathrm{F/sec} \,,$$

Table 1

Computer Program Input Information.

Problem Variable	Computer Variable	Scaled Variable
$\frac{dT_{s1}}{d\tau}$	$\dot{T}$	$[0.48\,\dot{T}]$
$T_{s_1}, T_{s_3}, T_{s_4}$	$T_{s_1}, T_{s_3}{}^*, T_{s_4}{}^*$	$\left[\frac{T_{s_1}}{10}\right]$
$T^4_{s_1}, T^4_{s_3}, T^4_{s_4}$	$T^4_{s_1}, T^4_{s_3}{}^*, T^4_{s_4}{}^*$	$\left[10^{-4}\left(\frac{T_{s_1}}{10}\right)^4\right]$
θ	ωt	$[\omega t]$
Equation Constants and Coefficients	**Problem Constants**	**Value**
A_1	Q_{AP}	15.38 BTU/hr
B_1	q_{int}	64.12 BTU/hr
E_1	$\rho_{sp}\alpha_s F_v A_p S$	48.33 BTU/hr
$F_1(T^4_{p_s})$	$(F_{ps})_{gr} A_s \sigma (T^4_{ps})$	139.50 BTU/hr
C_1	$\epsilon_s F_\epsilon A_s E_\epsilon$	63.44 BTU/hr
D_1	$\alpha_s F_p A_p S$	48.33 BTU/hr
F_1	$(F_{ps})_{gr} A_s \sigma$	0.1557×10^{-8} BTU/hr(°R)^4
G_1	$\epsilon_s A_s \sigma$	0.2184×10^{-8} BTU/hr(°R)^4
$(F + G)_1$	$\sigma[(F_{ps})_{gr} A_s + \epsilon_s A_s]$	0.3741×10^{-8} BTU/hr(°R)^4
$\frac{1}{R_{cond}}$	$\frac{\Delta X}{KA}$	0.5117 BTU/hr °F
$\frac{1}{R_{rad\ int}}$	$F_{14} A_1 \sigma, F_{15} A_1 \sigma, F_{17} A_1 \sigma$	$0.3988 \times 10^{-8}, 0.3551 \times 10^{-8}, 0.8915 \times 10^{-8}$
WC_p	WC_p	4.8 BTU/°F
T_5	T_{s5}	5.20 °R
T_6	T_{s6}	5.20 °R
T_{7A}	T_{7A}	5.20 °R

*Generated by Equation A1, written for thermal boundary sections 3 and 4.

and

$$\frac{T}{10} = 12.500\ [0.48\dot{T}]\ {}^{\circ}\mathrm{F/min.} \equiv \text{computer integration rate.}$$

To be compatible with the computer integration rate $\omega t = 0.48$ radians/orbit revolution,

$t = 1.6$ hrs. per orbit = 96 minutes/orbit.

Therefore, $[\omega] = 0.0655$ radians/min, flux generation rate.

Scaled Analog Diagram

In a technique identical to that above, three additional equations are evaluated, scaled, and mechanized. Table 2 lists the scaled coefficients for all four equations in terms of potentiometer and gain settings for the completely mechanized analog circuit (Figure A5). Figures A1, A2, A3, and A4 represent the earth flux generated for each node by the flux simulation circuits.

Table 2

Potentiometer Assignment Sheet.

P00–P59

DATE: SAMPLE PROBLEM

PROBLEM: THERMAL ANALYSIS CIRCUIT SSIS–1096

POT. NO. P	PARAMETER DESCRIPTION	SETTING STATIC CHECK	SETTING RUN NUMBER 1	POT. NO. P	PARAMETER DESCRIPTION	SETTING STATIC CHECK	SETTING RUN NUMBER 1
00	Solar Face Temp.	.5200	.5200	30	Scaling (gain = 12.5)	.5000	.5000
01	Aft Cover Temp.	.5200	.5200	31	Initial Temp.-Sur. 4	.5000	.5000
02	Tube Temp.	.5200	.5200	32			
03	Plotter	——	.5000	33	Conduction-Skin	.1022	.1022
04	IR Flux $f(F_e)$ Control 3	.5249	.5249	34			
05	Plotter-X Drive	——	.0096	35	Initial Temp.-Sur. 3	.5000	.5000
06	Sur. 1 $q_{rad\ int}$	.03998	.03998	36	Q Internal Sur. 3	.2673	.2673
07	Sur. 1 $q_{rad\ int}$	.03551	.03551	37	A_s Flux-Control-Sur. 3	.0595	.0595
08	Sur. 1 $q_{rad\ int}$	.08915	.08915	38	A_s Flux-Sur. 3 (α_s)	.2680	.2680
09				39	Conduction-Skin 3	.2044	.2044
10	Scaling (gain = 12.5)	.5000	.5000	40			
11	Initial Temp.-Sur. 1	.5000	.5000	41			
12	A_s Flux Control-Sur. 1	.0083	.0083	42			
13				43			
14	IR Flux Control-Sur. 1	.0900	.0900	44			
15	Sur. 2 $q_{rad\ int}$	.03998	.03998	45			
16	Initial Condition	.1000	.1000	46	Conduction-Skin	.1022	.1022
17	Sur. 2 $q_{rad\ int}$	.03551	.03551	47			
18	IR Flux Control-Sur. 3	.0456	.0456	48	Conduction-Skin	.1022	.1022
19	IR Flux $f(F_e)$ Control 2	.8830	.8830	49			
20	Scaling (gain = 12.5)	.5000	.5000	50			
21	Initial Temp.-Sur. 2	.5000	.5000	51			
22	A_s Flux-Sur. 2 (α_s)	.2680	.2680	52			
23	IR Flux Control-Sur. 2	.0864	.0864	53			
24	A_s Flux Control-Sur. 2	.0126	.0126	54			
25	IR Flux Control-Sur. 4	.0456	.0456	55			
26	IR Flux $f(F_e)$ Control 4	.5249	.5249	56			
27	A_s Flux Control-Sur. 4	.0456	.0456	57			
28	A_s Flux Control-Sur. 4	.7225	.7225	58			
29				59			

Table 2 (Continued)

Potentiometer Assignment Sheet.

Q00–Q59

DATE: SAMPLE PROBLEM **PROBLEM:** THERMAL ANALYSIS CIRCUIT SSIS–1096

POT. NO. Q	PARAMETER DESCRIPTION	SETTING STATIC CHECK	SETTING RUN NUMBER 1	POT. NO. Q	PARAMETER DESCRIPTION	SETTING STATIC CHECK	SETTING RUN NUMBER 1
00	Plotter	———	.5000	30			
01	Plotter	———	.5000	31	Conduction-Skin 4	.2044	.2044
02	Plotter	———	.5000	32	Q Internal-Sur. 4	.2673	.2673
03	Plotter	———	.5000	33	IR Emission-Sur. 4	.3742	.3742
04	IR Flux $f(F_e)$ Control 1	.4225	.4225	34	Plotter	———	.5000
05	A_s Flux $f(F_p)$ Control 1	.2720	.2720	35	A_s Flux $f(F_p)$ Control 2	.2567	.2567
06	Sur. 3 $q_{rad\ int}$	.03998	.03998	36	IR Emission-Surf. 3	.3742	.3742
07	Sur. 3 $q_{rad\ int}$	.03551	.03551	37	Scaling (gain =12.5)	.5000	.5000
08	Sur. 3 $q_{rad\ int}$	.08915	.08915	38	A_s Flux Control-Sur. 3	.0101	.0101
09	A_s Flux-Sur. 1 (α_s)	.2680	.2680	39	A_s Flux $f(F_p)$ Control 3	.2605	.2605
10	IR Flux-Sur. 1 (ϵ)	.0800	.0800	40	Ave. Temp. Divider	———	.3000
11	Conduction-Skin 1	.2044	.2044	41			
12	Q Internal-Sur. 1	.2673	.2673	42			
13	IR Emission-Sur. 1	.3741	.3741	43			
14	A_s Flux Control Sur. 1	.7700	.7700	44			
15	Sin & Cos Generator	———	.0655	45			
16	Sin & Cos Generator	———	.0655	46	Conduction	.1022	.1022
17				47	Sur. 4 $q_{rad\ int}$	.03998	.03998
18	Sur. 2 $q_{rad\ int}$	.08915	.08915	48	Sur. 4 $q_{rad\ int}$	.03551	.03551
19	IR Flux-Sur. 3 (ϵ)	.0800	.0800	49	Sur. 4 $q_{rad\ int}$	.08915	.08915
20	IR Flux-Sur. 2 (ϵ)	.0800	.0800	50			
21	Conduction-Skin 2	.2044	.2044	51			
22	Q Internal-Sur. 2	.2673	.2673	52			
23	IR Emission-Sur. 2	.3741	.3741	53			
24	A_s Flux Control Sur. 2	.7700	.7700	54			
25	A_s Flux-Sur. 4 (α_s)	.2680	.2680	55			
26	IR Flux-Sur. 4 (ϵ)	.0800	.0800	56			
27	A_s Flux $f(F_p)$ Control 4	.2630	.2630	57			
28	A_s Flux Control-Sur. 4	.9100	.9100	58			
29				59			

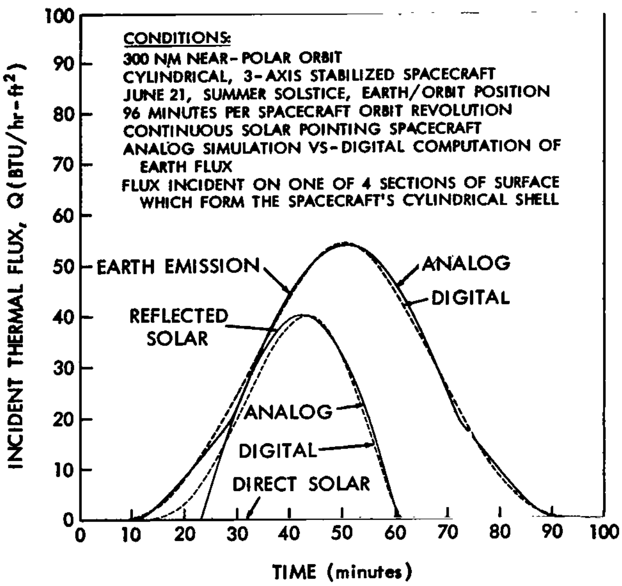

Figure A1—Incident thermal flux to spacecraft surface section 1.

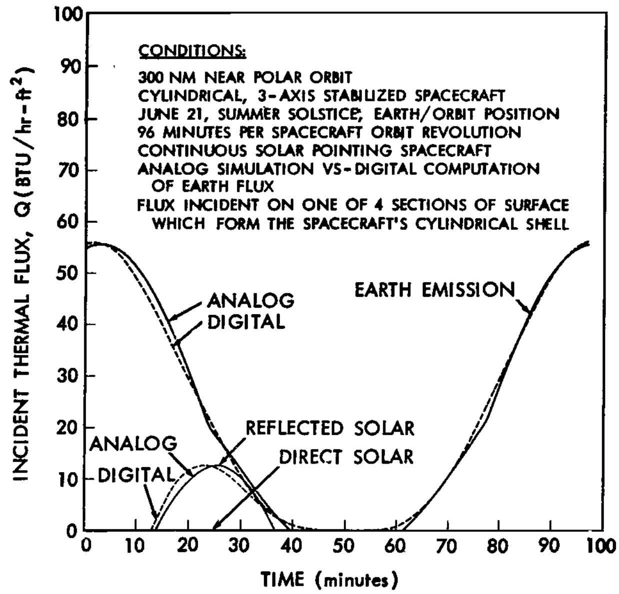

Figure A2—Incident thermal flux to spacecraft surface section 2.

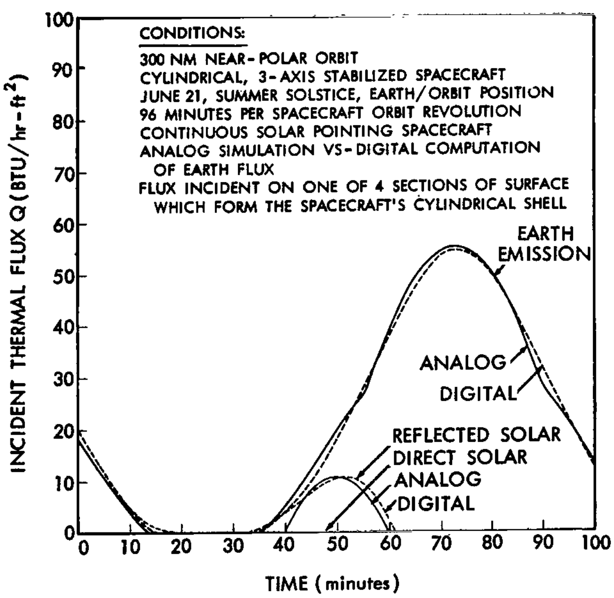

Figure A3—Incident thermal flux to spacecraft surface section 3.

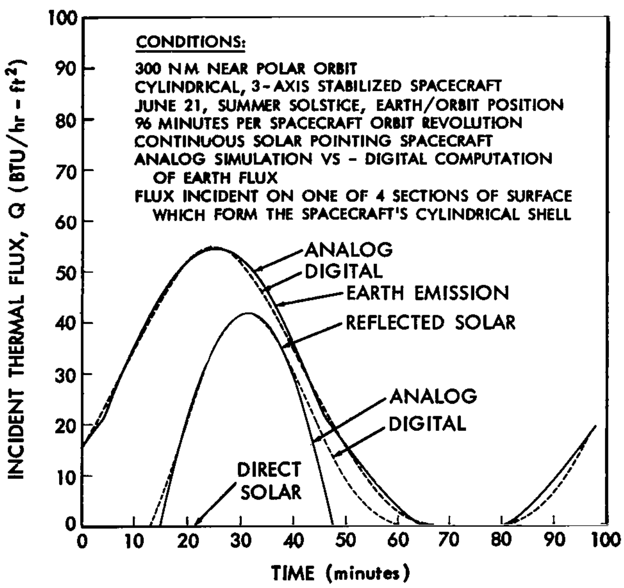

Figure A4—Incident thermal flux to spacecraft surface section 4.

NASA-Langley, 1967 G-749

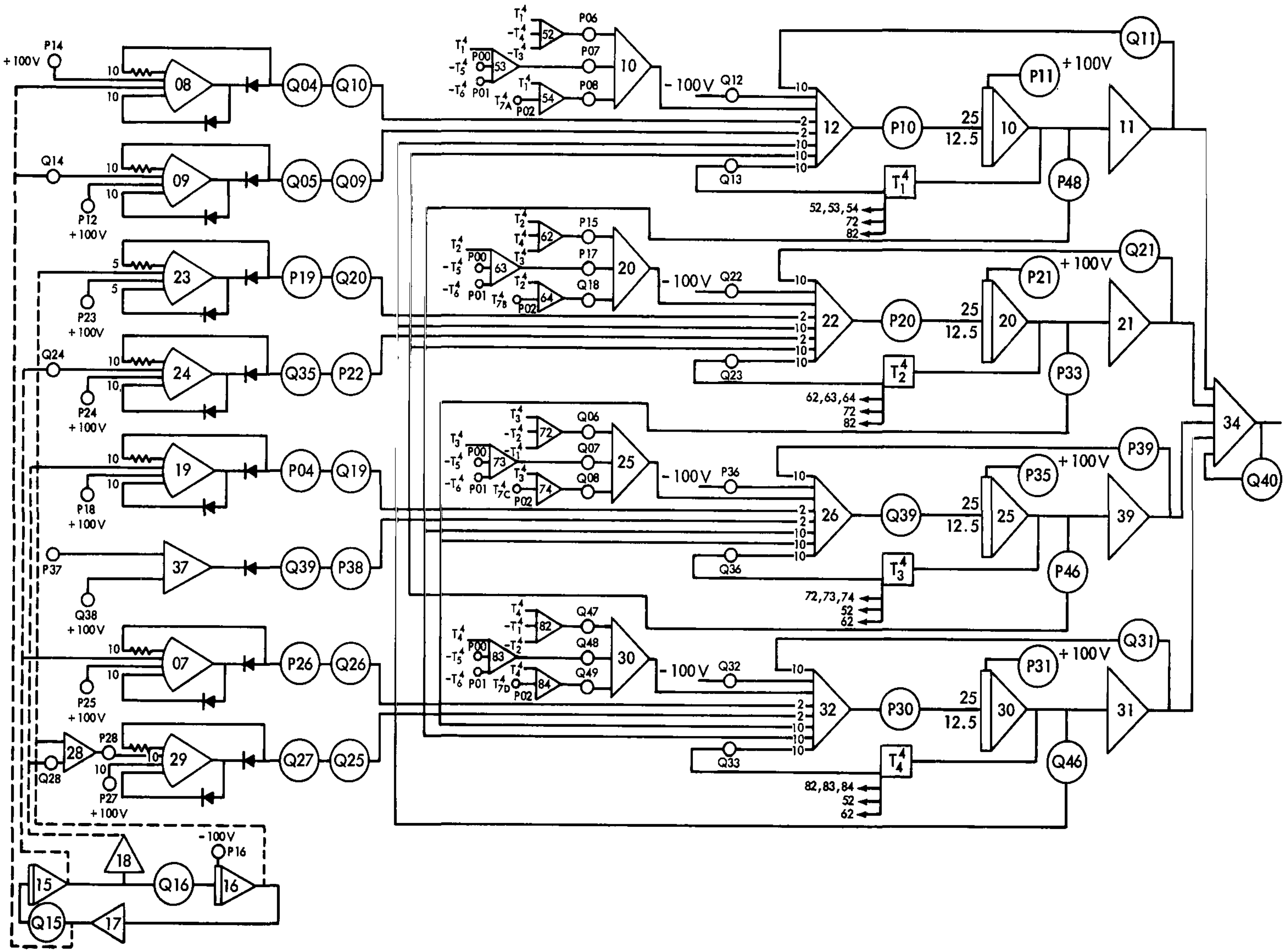

Figure A5—Complete thermal analysis analog circuit diagram.

"The aeronautical and space activities of the United States shall be conducted so as to contribute . . . to the expansion of human knowledge of phenomena in the atmosphere and space. The Administration shall provide for the widest practicable and appropriate dissemination of information concerning its activities and the results thereof."

—NATIONAL AERONAUTICS AND SPACE ACT OF 1958

NASA SCIENTIFIC AND TECHNICAL PUBLICATIONS

TECHNICAL REPORTS: Scientific and technical information considered important, complete, and a lasting contribution to existing knowledge.

TECHNICAL NOTES: Information less broad in scope but nevertheless of importance as a contribution to existing knowledge.

TECHNICAL MEMORANDUMS: Information receiving limited distribution because of preliminary data, security classification, or other reasons.

CONTRACTOR REPORTS: Technical information generated in connection with a NASA contract or grant and released under NASA auspices.

TECHNICAL TRANSLATIONS: Information published in a foreign language considered to merit NASA distribution in English.

TECHNICAL REPRINTS: Information derived from NASA activities and initially published in the form of journal articles.

SPECIAL PUBLICATIONS: Information derived from or of value to NASA activities but not necessarily reporting the results of individual NASA-programmed scientific efforts. Publications include conference proceedings, monographs, data compilations, handbooks, sourcebooks, and special bibliographies.

Details on the availability of these publications may be obtained from:

SCIENTIFIC AND TECHNICAL INFORMATION DIVISION

NATIONAL AERONAUTICS AND SPACE ADMINISTRATION

Washington, D.C. 20546